Conversion of Lanthanide Glutarate Chlorides with Interstitial THF into Lanthanide Glutarates with unprecedented Topologies.

Ralph A. Zehnder,*[#] James Jenkins,[#] Matthias Zeller,[†] Christian Dempsey,[§] Stosh A. Kozimor,[$]
Gregory Jackson,[‡] Katherine Gilbert,[#] Matthew Smith[‡]

[#]Department of Chemistry and Biochemistry, [§]Department of Physics, [‡] Department of Biology,
Angelo State University, San Angelo, TX 76909, [$]Los Alamos National Laboratory, Los
Alamos, NM 87545, and [†]Department of Chemistry, Purdue University, West Lafayette, IN
47907.

ABSTRACT

Using slow diffusion methods at room temperature (RT), we obtained four isomorphous lanthanide glutarate chlorides, accommodating interstitial THF and water molecules, $[Ln_2(Glut)_2Cl_2(H_2O)_8]\cdot2H_2O\cdot THF$ **(1 - 4)**, with Ln = La (**1**), Ce (**2**), Pr (**3**), Nd (**4**). They assemble as 3-dimensional (3D) lanthanide (Ln) coordination polymers with LnO_{10} coordination

polyhedra. Their topology was elucidated to be a 4-coordinated **sql** net. **1 – 4** slowly dissolve in water liberating the entrapped THF molecules and reassemble as regular Ln-glutarate hydrates when the solution is deprived of THF and water by slow evaporation. The new products crystallize as $[Ln_2(Glut)_3(H_2O)_3]\cdot 5H_2O$ (**5** - **7**), with Ln = La (**5**), Ce (**6**), Pr (**7**), and $[Nd_2(Glut)_3(H_2O)_2]\cdot 3.5H_2O$ (**8**). **5 – 7** are isomorphous and crystallize as 3D-networks with two crystallographically independent LnO_{10} and LnO_9 coordination spheres that assemble into Ln_2O_{18} and Ln_2O_{16} polyhedra via edge sharing. Their topology has not previously been observed and was found to be a 3,4,4,5,6-coordinated 3,4,4,5,6T61 net. The known compound **8** crystallizes also as a 3D-network and is isomorphous to other previously described lanthanide glutarate hydrates. **8** has a 3,4,5-coordinated 3,4,5T202 net topology, which has not been determined before.

INTRODUCTION

Metal Organic Framework compounds incorporating lanthanide metal centers (Ln-MOFs) have gained significant interest in recent years. This has resulted in a growing number of coordination networks with extended coordination numbers and rather unique topologies.[1-7] Studying *f*-element MOFs has contributed to the advancement of fundamental knowledge in *f*-element chemistry.[8-14] Consequently, a growing number of porous materials, equipped with customized interstices, interesting topologies, and the ability to host various guest entities have lately been reported in the literature.[3, 5, 6, 15-17]

We previously reported a neodymium terephthalate glutarate, $[Nd_2(Glut)_2(TP)(H_2O)_4]\cdot 17H_2O$, which assembles as a 3D-coordination polymer, crystallizing in the orthorhombic crystal system with space group *C*mcm.[18] It's topology was elucidated to be a

4,5-coordinated **fsc**-4,5-Cmmm network. Our efforts to extend its synthesis, hydrothermal reaction of neodymium oxide, terephthalic acid and glutaric acid at 170 °C, to other lanthanides remained however unsuccessful. Employment of slow diffusion methods using the lanthanide chlorides and the carboxylate anions at room temperature (RT), on the other hand, enabled us to create the targeted compounds beyond Nd^{3+}, including La^{3+}, Ce^{3+}, Pr^{3+}, and Sm^{3+}. The dicarboxylic acids were first converted into their sodium salts using NaOH, dissolved in mixtures of H_2O, THF and EtOH and reacted with aqueous $LnCl_3 \cdot xH_2O$ solutions via slow diffusion in scintillation vials. Some of these experiments afforded another THF containing coordination network as a regular by-product, $[Ln_2(Glut)_2Cl_2(H_2O)_8] \cdot 2H_2O \cdot THF$. Interestingly, the crystallographic properties of these compounds are very similar to those of the originally targeted structures, which prompted us to pursue their deliberate synthesis to test their potential as MOF model compounds for the *f*-elements. Adjusting the original slow diffusion experiments to proceed without the terephthalate resulted in the production of well-formed single crystals of $[Ln_2(Glut)_2Cl_2(H_2O)_8] \cdot 2H_2O \cdot THF$.

EXPERIMENTAL SECTION

General Remarks.

Chemicals used as starting materials were purchased from Sigma Aldrich (terephthalic acid, THF), Alfa Aesar (glutaric acid, $LaCl_3 \cdot xH_2O$, $PrCl_3 \cdot xH_2O$, $NdCl_3 \cdot xH_2O$), Acros Organics ($CeCl_3 \cdot 7H_2O$), Calbiochem (OmniPur Ethanol 200 proof), and were used without further purification.

Synthesis and Characterization.

Synthesis of lanthanide glutarate chlorides with interstitial THF molecules, $[Ln_2(Glut)_2Cl_2(H_2O)_8] \cdot 2H_2O \cdot THF$ (1 - 4), with Ln = La (1), Ce (2), Pr (3), Nd (4):

A 7 mL scintillation vial, nearly completely filled with $H_2O/THF/EtOH$, was lowered into a 50 mL Falcon PPE conical tube. A solution of Na_2Glut (170 mmol/L) in a 1:1:1 mixture of $H_2O/THF/EtOH$ was carefully filled into the 50 mL conical tube outside of the 7 mL vial until the scintillation vial was completely covered. ~1 mL of a saturated aqueous $LnCl_3$ solution was carefully placed at the bottom of the 7 mL vial using a pipette or syringe. The reagent free solvent mixture at the top of the scintillation vial serves as a buffer zone to ensure slow diffusion of reagents. The outer conical tube was then capped and left undisturbed. Within two weeks well-developed crystals grew in form of thin needles. The majority of the crystals developed at the rim of the scintillation vial. Thus, at the interface between the solvent mixture inside the scintillation vial and the ligand solution surrounding the vial. Eventually crystals dropped to the bottom of the scintillation vial and could be easily harvested by lifting out the scintillation vial from the conical tube. The structures were elucidated via single crystal X-ray diffraction yielding isomorphous **1** - **4**. Crystals for the X-ray experiments were directly taken from the samples suspended in the original $H_2O/THF/EtOH$ solvent mixtures. Drying of the material in air at room temperature, e.g. in open vials in the drag of a fume hood, led to loss of crystallinity as indicated by featureless powder-XRD patterns. Elemental analysis results are consistent either with the

original product or after the loss of THF and/or various amounts of water. FT-IR spectroscopy data reported are of air-dried samples.

Anal. calcd. for $La_2C_{14}O_{19}H_{40}Cl_2$ (**1**) C, 19.53%; H, 4.68%. Found C, 16.84%; H, 3.46%. After adjustment for solvent loss (THF and $4H_2O$), anal. calcd.: C, 16.74%; H, 3.37%. FT-IR: 3335 (br), 3230 (br), 2983 (w), 2957 (w), 2921 (w), 2888 (w), 1646 (s), 1635 (w), 1586 (s), 1539 (vs), 1511 (w), 1488 (w), 1443 (s), 1429 (vs), 1417 (s), 1347 (s), 1320 (w), 1294 (s), 1274 (s), 1219 (s), 1161 (w), 1059 (s), 964 (w), 933 (w), 897 (w), 867 (w), 800 (w), 745 (s), 624 (s), 603 (s), 525 (s), 484 (s).

Anal. calcd. for $Ce_2C_{14}O_{19}H_{40}Cl_2$ (**2**) C, 19.47%; H, 4.67%. Found C, 15.38%; H, 4.11%. After adjustment for solvent loss (THF), anal. calcd.: C, 15.17%; H, 4.07%. FT-IR: 3300 (br), 3200 (br), 2960 (w), 2880 (w), 1620 (vs), 1530 (vs), 1420 (vs), 1340 (vs), 1290 (s), 1220 (w), 1060 (s), 1020 (s), 964 (s), 862 (s), 742 (s), 685 (s), 598 (s).

Anal. calcd. for $Pr_2C_{14}O_{19}H_{40}Cl_2$ (**3**) C, 19.44%; H, 4.66%. Found C, 20.50%; H, 3.87%. FT-IR: 3300 (br), 3190 (br), 2960 (w), 2890 (w), 2190 (w), 2110 (w), 1620 (vs), 1530 (vs), 1430 (vs), 1420 (vs), 1350 (vs), 1290 (vs), 1220 (s), 1060 (s), 1020 (s), 964 (w), 933 (w), 889 (s), 862 (s), 742 (s), 687 (s), 594 (s).

Anal. calcd. for $Nd_2C_{14}O_{19}H_{40}Cl_2$ (**4**) C, 19.29%; H, 4.62%. Found C, 22.96%; H, 3.32%. After adjustment for solvent loss ($8H_2O$), anal. calcd.: C, 23.11%; H, 3.32%. FT-IR: 3300 (br), 3210 (br), 2980 (w), 2310 (w), 2110 (w), 1640 (w), 1570 (vs), 1540 (w), 1440 (vs), 1400 (vs), 1350 (vs), 1320 (s), 1290 (w), 1270 (s), 1200 (w), 1160 (w), 1070 (w), 1060 (s), 970 (w), 899 (s), 796 (w), 744 (s), 582 (w), 536 (w).

Synthesis of lanthanide glutarate hydrates, [Ln$_2$(Glut)$_3$(H$_2$O)$_3$]•5H$_2$O (5 - 7), with Ln = La (5), Ce (6), Pr (7), and [Nd$_2$(Glut)$_3$(H$_2$O)$_2$]•3.5H$_2$O (8):

Dissolution of [Ln$_2$(Glut)$_2$Cl$_2$(H$_2$O)$_8$]·2H$_2$O·THF **(1 - 4)** in deionized (DI) -H$_2$O and slow evaporation of residual THF and water in the drag of a fume hood resulted in crystallization of **5 - 7**, which grew as isomorphic single crystals in form of small blocks, and **8**, which formed thin needles. The resulting materials containing **5 - 8** were harvested from the remaining aqueous solution and transferred into small scintillation vials (7 ml), and rinsed with DI-H$_2$O. Their structures were elucidated via single crystal X-ray diffraction. Small samples of the remaining materials were dried in a laboratory oven at 35 °C and were then homogenized using a ball pestle and shaker, and used for elemental and FT-IR spectroscopy analyses. Crystals partially desolvate upon drying. Elemental analysis results indicate loss of water upon air-drying of samples. We were unable to isolate **8** as purely as **5 - 7**.

Anal. calcd. for La$_2$C$_{15}$O$_{20}$H$_{34}$ **(5)** C, 22.18%; H, 4.22%. Found C, 25.51%; H, 3.08%. After adjustment for solvent loss (6H$_2$O), anal. calcd.: C, 25.59%; H, 3.15%. FT-IR: 3309 (br), 3219 (br), 2952 (w), 2920 (w), 2845 (w), 1653 (s), 1646 (s), 1636 (s), 1586 (s), 1540 (m), 1506 (w), 1488 (w), 1472 (w), 1453 (s), 1443 (s), 1417 (w), 1403 (w), 1346 (w), 1319 (w), 1274 (m), 1199 (w), 1058 (w), 745 (sh), 680 (br), 545 (br).

Anal. calcd. for Ce$_2$C$_{15}$O$_{20}$H$_{34}$ **(6)** C, 22.12%; H, 4.21%. Found C, 24.46%; H, 3.06%. After adjustment for solvent loss (5H$_2$O), anal. calcd.: C, 24.86%; H, 3.34%. FT-IR: 3309 (br), 3219 (br), 2948 (w), 2917 (w), 2844 (w), 1653 (s), 1646 (s), 1636 (s), 1586 (w), 1534 (vs), 1495 (w),

1470 (w), 1455 (s), 1428 (s), 1411 (w), 1403 (w), 1349 (w), 1317 (w), 1288 (m), 1270 (m), 1196 (m), 1157 (w), 1058 (w), 815 (w), 660 (br), 561 (br).

Anal. calcd. for $Pr_2C_{15}O_{20}H_{34}$ (**7**) C, 22.07%; H, 4.20%. Found C, 25.55%; H, 2.99%. After adjustment for solvent loss ($6H_2O$), anal. calcd.: C, 25.44%; H, 3.13%. FT-IR: 3321 (br), 3235 (br), 3026 (w), 2922 (m), 2849 (w), 1653 (m), 1646 (m), 1636 (s), 1582 (m), 1562 (s), 1548 (vs), 1540 (vs), 1535 (vs), 1495 (m), 1464 (w), 1454 (vs), 1429 (vs), 1418 (vs), 1404 (vs), 1348 (m), 1317 (m), 1288 (m), 1272 (m), 1198 (w), 1159 (w), 1058 (m), 819 (w), 748 (w), 699 (s), 667 (s).

Anal. calcd. for $Nd_4C_{30}O_{35}H_{58}$ (**8**) C, 23.16.%; H, 3.76%. Found C, 23.94%; H, 3.25%. After adjustment for solvent loss ($4H_2O$), anal. calcd.: C, 24.29%; H, 3.40%. FT-IR: 3321 (br), 3235 (br), 3063 (w), 3028 (w), 2926 (m), 2850 (w), 1653 (w), 1646 (w), 1635 (w), 1582 (sh), 1562 (vs), 1549 (vs), 1539 (vs), 1532 (vs), 1507 (m), 1495 (m), 1464 (m), 1452 (vs), 1436 (vs), 1422 (vs), 1418 (vs), 1378 (w), 1354 (w), 1317 (m), 1273 (m), 1158 (w), 1061 (w), 755 (w), 698 (m), 643 (w).

Topological Analyses.

Topological analyses were performed by the ToposPro Team using the ToposPro program package and the TTD collection of periodic network topologies.[19]

The RCSR three-letter codes were used to designate the network topologies.[20] Those nets that are absent in the RCSR are designated with the Topos NDn nomenclature, where N is a sequence of coordination numbers of all non-equivalent nodes of the net, D is periodicity of the net (D=M, C, L, T for 0-,1-,2-,3-periodic nets), and n is the ordinal number of the net in the set of all non-isomorphic nets with the given ND sequence.[21]

Coordination mode or connectivity of ligands to metal atoms in coordination compounds is characterized with the notation L^{mbtkpghon}. The symbol L is a letter M, B, T, K, P, G, H, O, or N designating the number (1, 2, 3, …, 9) of donor atoms that are coordinated to the metal atoms (A). Integers m, b, t, ... are equal to the number of metal atoms connected to one, two, three, ... donor atoms.[22]

X-ray Structure Determination.

Intensity data for crystals of compounds **2**, **3**, **5**, and **6** were collected on a Bruker D8 Quest single-crystal X-ray diffractometer equipped with a complementary metal–oxide–semiconductor (CMOS) detector and an I-μ-S microsource MoK$_\alpha$ X-ray tube (λ= 0.71073 Å). The data for **1** and **4** were collected using a Bruker AXS APEXII CCD diffractometer featuring a sealed tube MoK$_\alpha$ X-ray source (λ= 0.71073 Å) with graphite monochromator. Data for crystals of compound **7** were collected on a Nonius Kappa CCD diffractometer with a sealed tube MoK$_\alpha$ X-ray source (λ= 0.71073 Å) with graphite monochromator. Data collection and initial indexing and cell refinement were handled using Nonius Collect software.[23] The XRD data for **8** were collected with a Rigaku Rapid II curved image plate diffractometer using the dTrek option of the CrystalClear software.[24] Single crystals for all compounds were mounted on Mitegen micromesh mounts using a trace of mineral oil and cooled in-situ to 100(2) K for data collection. For compounds **1-6**, frames were collected, reflections were indexed and processed, and the files scaled and corrected for absorption using APEX2. Data for both **7** and **8** were processed using HKL3000[25] and corrected for absorption and scaled using Scalepack.[25] Space groups for all structures were assigned using XPREP within the SHELXTL suite of programs[26] and the structures were solved by either direct methods, Patterson methods using ShelXS-97,[27] or by

isomorphous replacement based on known structures. Structures were refined by full matrix least squares against F^2 with all reflections using Shelxl2013 or 2014[28] using the graphical interface Shelxle.[29, 30] H atoms attached to carbon atoms were positioned geometrically and constrained to ride on their parent atoms, with carbon hydrogen bond distances of 0.99 Å with $U_{iso}(H) = 1.2$ $U_{eq}(C)$.

Structures **1-4** are isomorphous and were refined using a common structural model. THF molecules are disordered in place over four symmetry equivalent positions. The ADPs of THF atoms were subjected to a similarity restraint (SIMU 0.01 in Shelxl2014) and to a rigid bond restraint (RIGU 0.01 in Shelxl2014). Equivalent C-C and C-O distances within the THF molecule were restrained to be similar (SADI in Shelxl2014). Water H atom positions were restrained based on hydrogen bonding considerations.

Structures **5-7** are isomorphous and were refined using a common structural model. Crystals under investigation for all three compounds were found to be non-merohedrically twinned by a 180° rotation around the reciprocal b-axis. For **5** and **6**, the orientation matrices for the two components were identified using the program Cell_Now. The two components were integrated using Saint and corrected for absorption using twinabs, resulting in the following statistics:

Compound **5**:

15127 data (4735 unique) involve domain 1 only, mean I/sigma 62.3

15168 data (4731 unique) involve domain 2 only, mean I/sigma 57.1

9751 data (3853 unique) involve 2 domains, mean I/sigma 80.7

Compound **6**:

6215 data (2563 unique) involve domain 1 only, mean I/sigma 60.1

6180 data (2552 unique) involve domain 2 only, mean I/sigma 50.9

12017 data (4971 unique) involve 2 domains, mean I/sigma 73.

The exact twin matrices identified by the integration program were found to be -0.99989 0.00032 0.00013, 0.47322 0.99995 0.34697, -0.00026 -0.00013 -1.00005 for compound **5** and -1.00000 0.00003 -0.00002, 0.47443 1.00002 0.34789, 0.00004 -0.00015 -1.00002 for compound **6**. The structures were solved using direct methods with only the non-overlapping reflections of component 1 and refined using the hklf 5 routine with all reflections of component 1 (including the overlapping ones), resulting in BASF values of 0.4530(5) for **5** and 0.4108(9) for **6**. The R_{int} values given for **5** and **6** are for all reflections and are based on agreement between observed single and composite intensities and those calculated from refined unique intensities and twin fractions.[31]

For compound **7**, programs compatible with the diffractometer and HKL3000 lack the ability to simultaneously integrate more than one twin domain. With no data set obtainable through simultaneous integration of both twin domains, the data were instead handled as if not twinned, with only the major domain integrated, and converted into an hklf 5 type format hkl file after integration using the "Make HKLF5 File" routine as implemented in WinGX. The twin law and matrix were obtained using the program ROTAX as implemented in WinGX, yielding a twin matrix of -1 0 0, 0.472 1 0.345, 0 0 -1. The Overlap R1 and R2 values in the "Make HKLF5 File" routine used were 0.14, i.e. reflections with a discriminator function less or equal to overlap radius of 0.14 were counted as overlapped, all others as single. The discriminator function used was the "delta function on index non-integrality". No reflections were omitted. No R_{int} value is obtainable for the hklf 5 type file using the WinGX routine.

For compounds **5** to **7** the water molecule of O19 is hydrogen bonded to its symmetry equivalent across an inversion center, inducing disorder of its hydrogen atoms and of H atoms of the neighboring water molecule of O16. Hydrogen atoms were refined as 1:1 disordered and their positions were restrained based on hydrogen bonding considerations. For compound **7**, due to the less than ideal handling of twinning several atoms showed signs of ill-defined ADPs, and atoms O1, C2, C5, O4, C10 and O8 were restrained to be close to isotropic.

Compound **8** is known[32, 33] and isotypic to its Ho, Er [34], Gd, Sm derivatives as well as the Dy and Tb analogues,[35, 36]. It is isomorphous to the structure of the Sm-derivative, previously solved in our laboratory, which we will report elsewhere along with the Ho and Gd species.

A chain of water molecules is systematically disordered across a crystallographic two-fold axis and its atoms are thus exactly half occupied. At one end of the chain inter-chain interactions prohibit the presence of the terminal water molecule for every second chain end, thus inducing one water molecule to be only one quarter occupied (O9B, refined occupancy ca 31.9%). A hydrogen bond at the center of the chain across a two fold axis, connecting symmetry equivalent water molecules, induces additional 1:1 disorder of two hydrogen atoms (H9B and H9C). Water H atoms were initially refined with restraints based on hydrogen bonding considerations. In the final refinement cycles H atoms of non-metal coordinated water molecules were constrained to ride on their respective water carrier atom. Complete crystallographic data, in CIF format, have been deposited with the Cambridge Crystallographic Data Centre. CCDC 1558519-1558526 contain the supplementary crystallographic data for this paper. This data can be obtained free of charge from The Cambridge Crystallographic Data Centre via

www.ccdc.cam.ac.uk/data_request/cif. Details on crystal data and structure refinement are listed in Table 1 and Table 2.

Figures displaying structural motifs were created using CrystalMaker® 9.2 for Mac as well as the ToposPro package.

FT-IR Spectroscopy.

IR spectra were collected on a PerkinElmer Spectrum 100 FT-IR Spectrometer using KBr pellets. Spectral resolution was typically 4 cm^{-1}, and average data sets included 32 scans. We used the following abbreviations to describe the observed vibration modes: very strong (vs), strong (s), medium (m), weak (w), shoulder (sh), and broad (br).

Elemental Analysis.

Elemental analysis (EA) was performed by Midwest Microlab using an Exeter Analytical CE-440 CHNOS elemental analyzer.

Table 1. Crystal Data and Summary of Data Collection and Refinement for Compounds **1 - 4**

Formula	[La$_2$(Glut)$_2$Cl$_2$(H$_2$O)$_8$]•2H$_2$O•THF (**1**)	[Ce$_2$(Glut)$_2$Cl$_2$(H$_2$O)$_8$]•2H$_2$O•THF (**2**)	[Pr$_2$(Glut)$_2$Cl$_2$(H$_2$O)$_8$]•2H$_2$O•THF (**3**)	[Nd$_2$(Glut)$_2$Cl$_2$(H$_2$O)$_8$]•2H$_2$O•THF (**4**)
Fw(g/mol	861.18	863.60	865.18	871.84
a (Å)	17.225(3)	17.1658(7)	17.1404(5)	17.0996(19)
b (Å)	8.8282(13)	8.7943(3)	8.7654(3)	8.7341(10)
c (Å)	19.500(3)	19.4113(6)	19.3513(6)	19.286(2)
α (°)	90	90	90	90
β (°)	90	90	90	90
γ (°)	90	90	90	90
V (Å^3)	2957.6(7)	2930.35(18)	2907.32(16)	2880.3(6)
Crystal system	Orthorhombic	Orthorhombic	Orthorhombic	Orthorhombic
Space group	Cmcm	Cmcm	Cmcm	Cmcm
Z	4	4	4	4
D$_c$ (Mg•m^{-3})	1.929	1.957	1.977	2.011
μ (mm^{-1})	3.105	3.325	3.572	3.827
F(000)	1696	1704	1712	1720
T (K)	100(2)	100(2)	100(2)	100(2)
Refln. Indep.	2496	2371	2890	2487
Refln. I>2σ(I)	2149	2014	2487	2393
R$_{int}$	0.0356	0.0296	0.0231	0.0380
R1 (I>2σ(I))	0.0210	0.0280	0.0204	0.0240
wR2 (I>2σ(I))	0.0486	0.0466	0.0358	0.0654

Table 2. Crystal Data and Summary of Data Collection and Refinement for Compounds **5 - 8**

Formula	[La$_2$(Glut)$_3$(H$_2$O)$_3$]•5H$_2$O (**5**)	[Ce$_2$(Glut)$_3$(H$_2$O)$_3$]•5H$_2$O (**6**)	[Pr$_2$(Glut)$_3$(H$_2$O)$_3$]•5H$_2$O (**7**)	[Nd$_2$(Glut)$_3$(H$_2$O)$_2$]•3.5H$_2$O (**8**)[32, 33]
Fw (g/mol)	812.24	814.66	816.24	1555.72
a (Å)	9.0304(7)	9.0090(8)	8.97150(10)	8.0266(5)
b (Å)	9.8208(8)	9.8135(10)	9.8738(2)	15.0249(11)
c (Å)	16.1928(12)	16.1296(15)	16.0593 (3)	19.5693(12)
α (°)	103.5646(19)	103.478(3)	103.3733(7)	90
β (°)	103,8727(18)	103,852(5)	103,9324(7)	92.853(5)
γ (°)	98.589(2)	98.566(3)	98.5385(14)	90
V(Å^3)=	1322.74(18)	1314.4(2)	1299.56(18)	2357.1(3)
Crystal system	triclinic	triclinic	triclinic	monoclinic
Space group	$P\overline{1}$	$P\overline{1}$	$P\overline{1}$	$C2$/c
Z	2	2	2	2
D$_c$(Mg•m^{-3})	2.039	2.058	2.086	2.192
μ (mm^{-1})	3.273	3.506	3.793	33.989
F(000)	796	800	804	1516
T(K)	100(2)	100(2)	100(2)	100(2)
Refln. Indep.	7829	10025	33891	2225
Refln. I>2σ(I)	7632	9619	30441	1881
R$_{int}$	0.0345	0.0536	0.0530	0.1052
R1 (I>2σ(I))	0.0211	0.0451	0.0594	0.0453
wR2 (I>2σ(I))	0.0614	0.1228	0.1553	0.1151

RESULTS AND DISCUSSION

Synthesis.

The treatment of $LnCl_3$ with sodium-glutarate (Na_2Glut) under the experimental conditions at room temperature afforded homogeneous crystalline products **1**, **2**, **3**, and **4**, who grew as small-sized single crystals in form of thin needles. Solvent molecules in **1** - **4** are only weakly bound and quite labile. Drying in air at room temperature, or even treatment of these products with water resulted in their transformation into non-crystalline material with featureless powder XRD patterns. Elemental analysis indicates loss of the interstitial THF molecule and some of the water molecules. They slightly dissolve in water and liberate entrapped THF by reassembling as the lanthanide glutarate hydrates **5**, **6**, **7**, and **8**, when the solution is concentrated by slow evaporation.

Solid State Structures.

$[Ln_2(Glut)_2Cl_2(H_2O)_8]\cdot2H_2O\cdot THF$, with $Ln = La$ (**1**), Ce (**2**), Pr (**3**), Nd (**4**):

1 - **4** are structural homologues and crystallize in the orthorhombic crystal system with space group *C*mcm. They assemble in 2D-layers of LnO_{10}-coordination polyhedra that infinitely stretch in the *b*-direction via edge sharing of LnO_{10} polyhedra through two oxygen atoms. Both O-atoms stem from glutarate carboxylate entities, positioned on opposite sides of the coordination polyhedron. In *c*-direction the LnO_{10}-polyhedra are bridged through glutarate units resulting in infinite chains. Both glutarate carboxylate groups dock to the Ln-metal centers in a κ^1-fashion for one oxygen atom and a μ_2-fashion for the second oxygen atom, connecting two adjacent Ln^{3+}-cations via edge sharing in *b*-direction and linking the Ln metal centers along the *c*-axis. This renders the coordination mode of glutarae in **1** - **4** to be K^{22} (Scheme **1**) and results

in the formation of infinite 1D-rods stretching along *b*-direction. The infinite linking of these rods via glutarate entities along the *c*-axis creates the 2D-layers in compounds **1 – 4**, which are further tied together in *a*-direction through ion-dipole interactions between Cl^--anions and hydrogen atoms belonging to water molecules inside the LnO_{10}-coordination sphere. The Cl^--anions are found in-between the *bc*-layers as showcased in Figure **1**. Additional intermolecular forces, supporting this arrangement, are provided by hydrogen bonds between the coordinating water molecules and interstitial water molecules, also positioned in-between these layers. The distance between *bc*-layers along *a*-direction is approximately 4 Å, which is significantly shorter than in the Nd-homologue of the original target structures, $[Nd_2(Glut)_2(TP)(H_2O)_4]\cdot17H_2O$, where layers are kept apart by the more spacious terephthalate (TP) entities at a distance of about 6 Å.[18] We are going to refer to $[Nd_2(Glut)_2(TP)(H_2O)_4]\cdot17H_2O$ and its homologues as the target structure(s) quite frequently, therefore we will represent them with **9** for simplicity. The other dimensions within the *bc*-layers are comparable to those of the neodymium glutarate terephthalate structures with ~3.5 Å in the *b*-direction (with Cl^- occupying these spaces in-between) and ~7 Å along the *c*-axis. While the interstices in the $[Nd_2(Glut)_2(TP)(H_2O)_4]\cdot17H_2O$ structures are filled with water molecules, the ones in **1 - 4** are filled out with THF, water molecules, and chloride ions. The THF molecules are held in place via hydrogen bonds between the THF-oxygen atoms and the interstitial water molecules, which are further hydrogen bonded to coordinating waters.
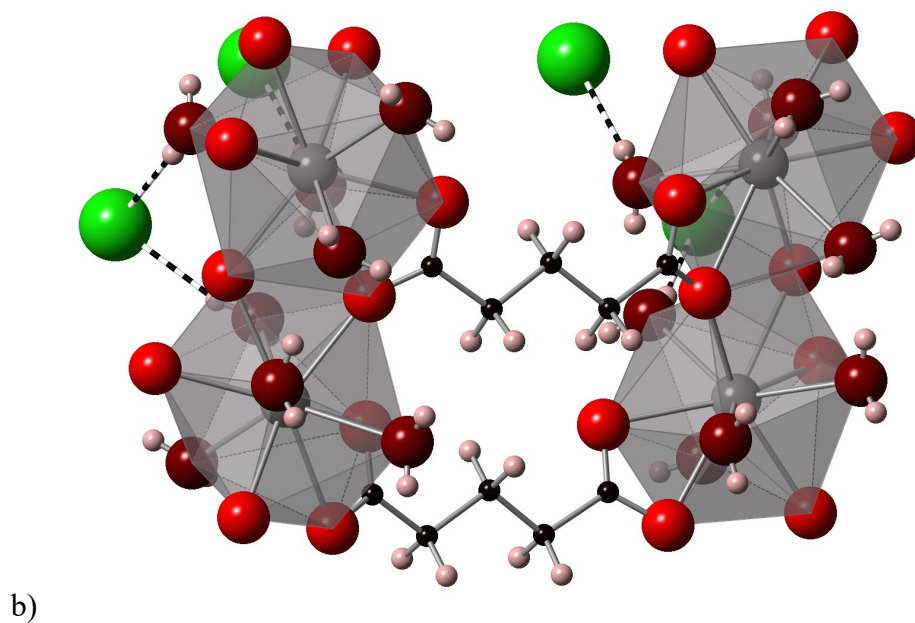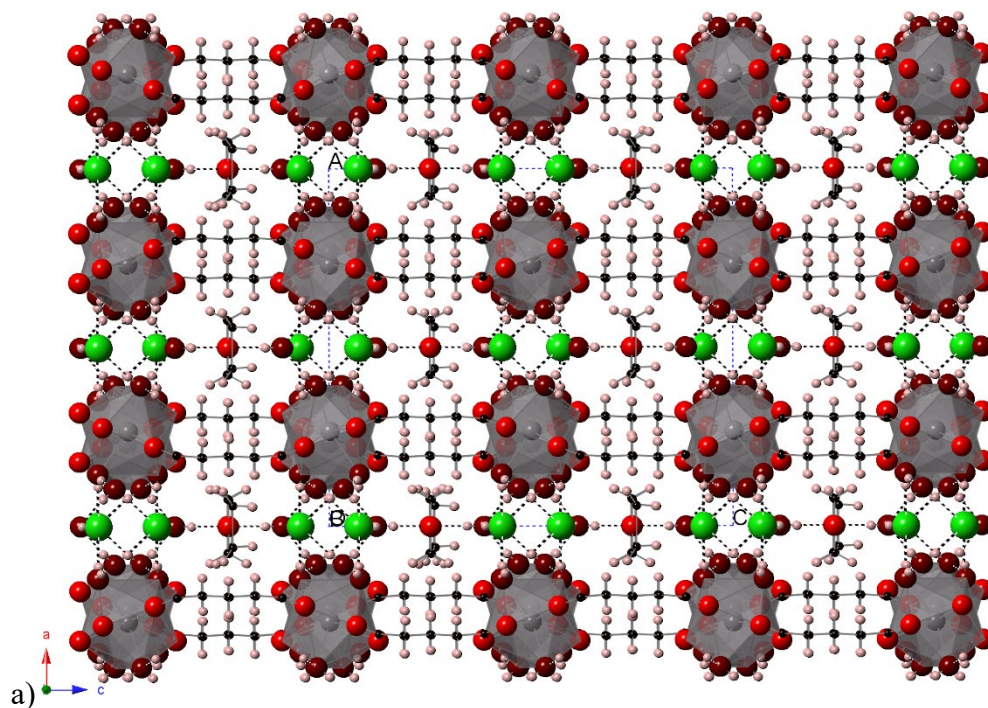
a)

b)

Figure 1. Structural arrangement of **2** (representative for **1** - **4**), forming 2D-layers in the bc-plane that are further connected along the a-axis via ion-dipole interactions facilitated by Cl⁻-ions and coordinating water molecules (red = O, maroon = O (from H_2O), white = H, green = Cl⁻, grey = Ln^{3+}, black = C). **a)** View onto the ac-plane with THF molecules held inside the interstices via H-bonds from interstitial H_2O, which is stabilized on its own via H-bonds to H_2O molecules that are part of the LnO_{10} coordination sphere. Cl⁻ is held in place via ion-dipole interactions stemming from coordinating H_2O. **b)** Tilted close-up view along the a-axis showing bridging of two Ln_2O_{18} polyhedra via the glutarate entities along the c-axis and the interactions between Cl⁻ and coordinating H_2O in a-direction.

The coordination polyhedra in **1 – 4** look identical to the ones in the neodymium glutarate terephthalate compounds (**9**) and assemble as bicapped square antiprisms. The dimensions inside the NdO_{10}-polyhedra in **4** and the ones in **9** compare extremely well. While 6 Nd-O bond distances are fairly identical in both coordination polyhedra, the two Nd-k^1O-distances in **4** are slightly longer (2.492 Å) than in **9** (2.419 Å). However, this effect is basically offset by a slight elongation of the capping O-atoms (one of the μ_2-oxygen atoms from the glutarate aligning with the *b*-axis) in **9** (2.746 Å) as compared to **4** (2.642 Å). The only physical difference between the coordination polyhedra in **9** and these new compounds is the replacement of the TP-carboxylate oxygen atoms with two individual water molecules within the coordination sphere of **1 – 4** (Figure **2**).
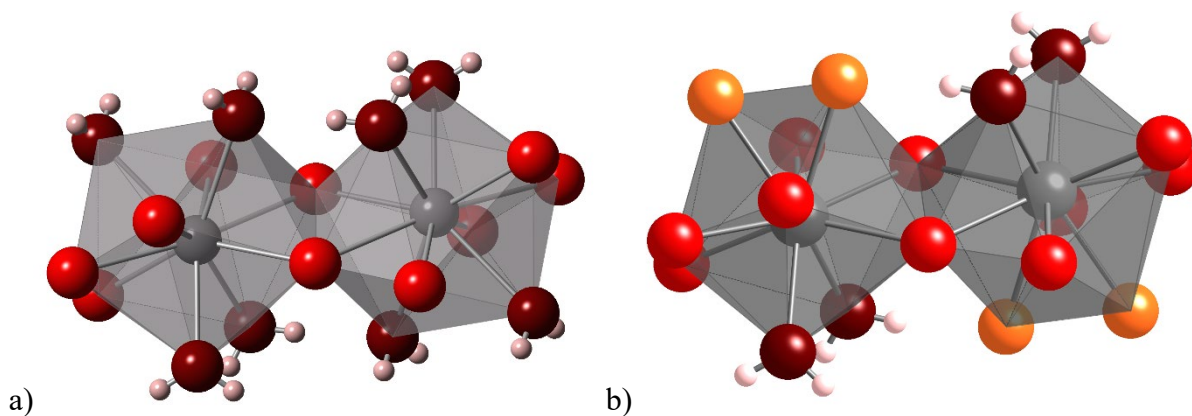
Figure 2. Comparison of the Ln_2O_{18} polyhedra in **2** (representative for **1 - 4**) **a)**, and the Ln_2O_{18} polyhedra as they assemble in the target structure, **b)** (red = O, maroon = O (from H_2O), orange = O from TP-entities in target structure) white = H, grey = Ln^{3+}).[18] The structural motifs of the polyhedra are identical with slight variations in bond distances. The only difference is the replacement of the terephthalate carboxylate O-atoms (orange) in **b)** with coordinating H_2O in **a)**.

The overall topological motif for **1 – 4** is a 4-coordinated **sql** net (Shubnikov tetragonal plane net),[20] with point symbol {4^4.6^2} as shown in Figure **3**. This is the most widespread 2D-topological type, reported for 8937 structures (organic, inorganic and metal-organic
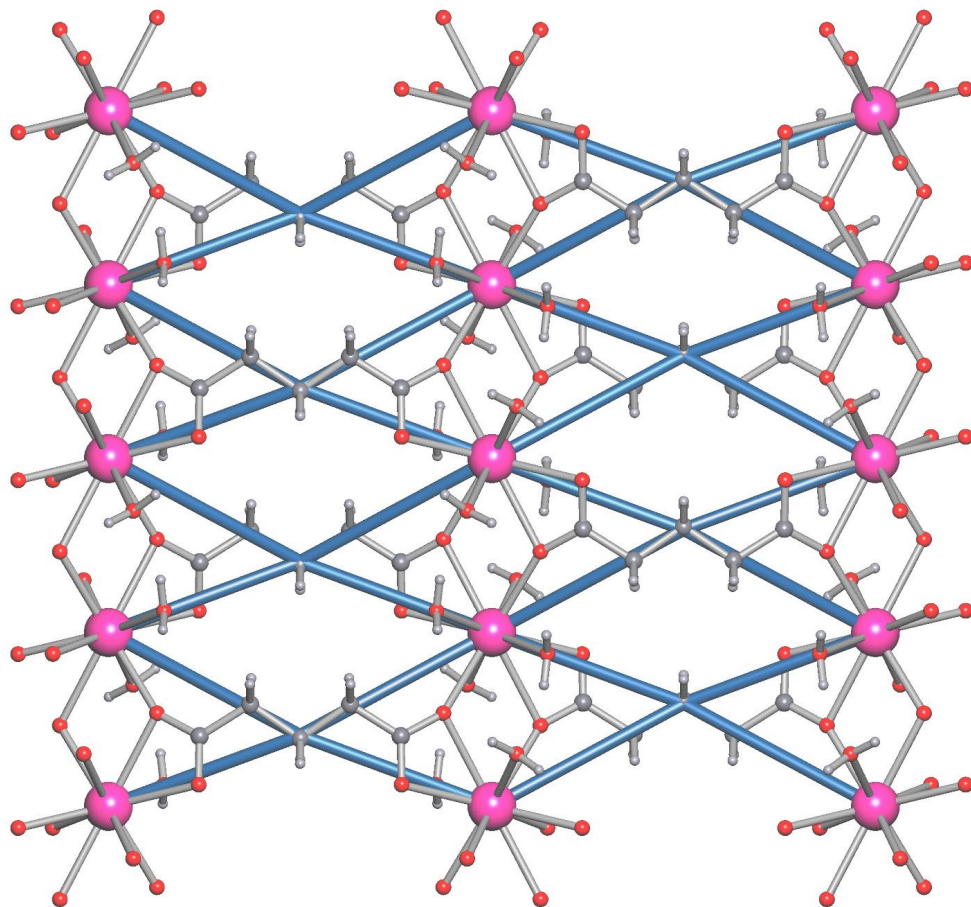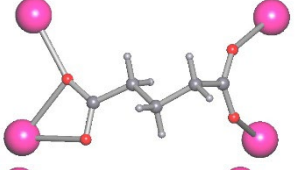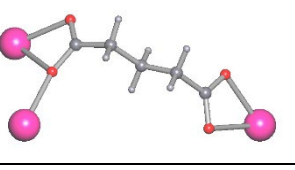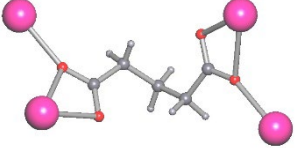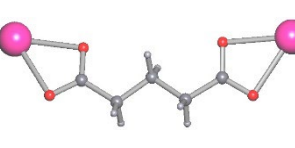
Figure 3. The **sql** underlying net (cyan) in the structures of **1** - **4**.

compounds according to the TTO collection of ToposPro). Of these 259 are coordination compounds containing glutarate, of which 68 are based on lanthanide elements as coordination centers. From the statistics of glutarate coordination modes for the 68 lanthanide structures, it can be seen that typical modes are K^{31} (tetradentate, five contacts with four metal atoms), K^{22} (tetradentate, six contacts with four metal atoms and coordination mode of glutarate in **1** - **4**), and K^{21} (tetradentate, four contacts with three metal atoms). A summary of these coordination modes is showcased in Scheme **1**. 19 of these lanthanide glutarate networks have the same coordination mode as **1** – **4**, which is the second by occurrence in the distribution.[35-38] Compound **8** is one of these and was previously reported by Serpaggi *et al*.[33] and Glowiak *et al*.[32]

CM	Figure	CM	Figure
K^{31}		K^{12}	
K^{22}		K^{02}	

Scheme 1. Glutarate linkers in compounds **1 – 4** occur with coordination mode K^{22}. Compounds **5 – 7** incorporate three independent glutarate anions with coordination modes K^{31}, K^{22}, and K^{12}. **8** exhibits two independent glutarate ions with coordination modes K^{22} and K^{12}. The target compound, $Nd_2(Glut)_2(TP)(H_2O)_4 \cdot 17H_2O$ (**9**), is comprised of glutarate and terephthalate units with coordination modes K^{22} and K^{02} Respectively.

$[Ln_2(Glut)_3(H_2O)_3] \cdot 5H_2O$ (**5 - 7**), with Ln = La (**5**), Ce (**6**), Pr (**7**):

5 - 7 Are isomorphous with identical structures and crystallize in the triclinic crystal system with space group $P\overline{1}$. The structures assemble as 3D-coordination polymers. Two crystallographically independent Ln^{3+}-metal centers are surrounded by 9 and 10 oxygen atoms respectively, forming Ln_2O_{16} and Ln_2O_{18} entities, in which two individual LnO_9 and LnO_{10} coordination polyhedra are connected via edge sharing respectively. Sets of crystallographically different Ln_2O_{16} and Ln_2O_{18} polyhedra are linked to each other via edge sharing in an alternating fashion as demonstrated in Figure 4. In the individual Ln_2O_{16} and Ln_2O_{18} polyhedra the two edge-sharing LnO_9 and LnO_{10} coordination spheres align in opposite directions along the *c*-axis.
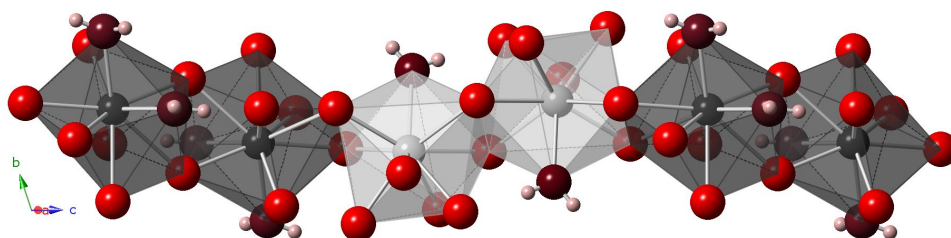

Figure 4. Alternating arrangement of crystallographically independent Ln_2O_{16} and Ln_2O_{18} polyhedra, connected via edge sharing in *c*-direction (red = O, maroon = O (from H_2O), white = H, dark grey = Ln^{3+}-1, light grey = Ln^{3+}-2). Ln_2O_{16} as well as Ln_2O_{18} polyhedra assemble from two individual LnO_9 and LnO_{10} coordination spheres via edge sharing of two O-atoms respectively.

The alternating assembly of Ln_2O_{16} and Ln_2O_{18} units (Figure **4**), stretching along the *c*-axis produces infinite chains. Scheme **2** showcases a structural fragment of these chains, which was found to be of a new type. The arrangement of these chains and their interlinkage by three independent glutarate spacers results in an unprecedented topology, which was determined to be a 3,4,4,5,6-coordinated 3,4,4,5,6T61 net, as shown in Figure **5**. The glutarate anions in **5** - **7** chelate with the individual coordination modes K^{31}, K^{22}, and K^{12} (Scheme **1**).
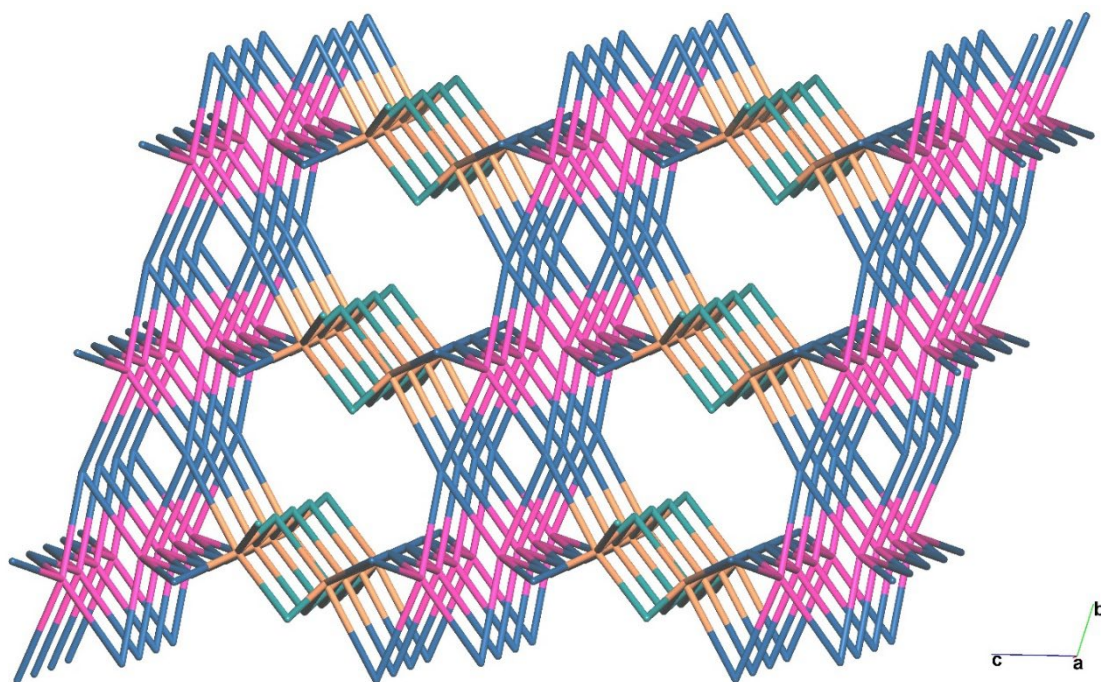
Figure 5. 3,4,4,5,6T61 underlying net in the structures of **5** - **7**. The underlying net contains 3-, 4-, 5- and 6-coordination nodes (cyan, blue, pink and orange colors, respectively).

LnO_{10} polyhedra (Ln-1, dark color) assemble from three carboxylate groups, docking to the Ln-1 metal center via κ^1-fashion for one oxygen atom and μ_2-fashion for the second oxygen atom. Two of the μ_2-coordinating O-atoms facilitate the edge sharing with the adjacent LnO_9 (Ln-2, light color) coordination polyhedron, while the third one connects to the adjacent Ln-1 central atom providing one O-atom for the edge sharing between two LnO_{10} coordination polyhedra. Two more glutarate entities dock to that LnO_{10} polyhedron with one oxygen atom

coordinating to that Ln metal center. One of them stems from a carboxylate connecting the two Ln-1 central atoms providing the second O-atom for the edge sharing of LnO_{10} polyhedra. The other carboxylate entity bridges the Ln-1 and the Ln-2 metal centers between LnO_{10} and LnO_9 polyhedra, providing one O-atom to each adjacent central atom respectively (K^{31} coordination mode). The remaining two vertices of the LnO_{10} polyhedron are occupied by coordinating water molecules.

The individual LnO_9 polyhedra (Ln-2, light color) amount from 4 oxygen atoms that are provided by two carboxylate groups, which are both aligned along the *a*-axis, docking on opposite sides of the Ln^{3+} metal center. One of these O-atoms participates in the edge-sharing of these Ln_2O_{16} polyhedra. Here, only one water molecule is part of the coordination sphere per Ln^{3+}, and the remaining 4 O-atoms stem from 4 different carboxylate groups, of which two are taking part in the edge sharing between LnO_9 and LnO_{10} polyhedra and one provides the second edge sharing O-atom between adjacent LnO_9 polyhedra. The forth O-atom is provided by a bridging carboxylate unit towards the adjacent Ln-1 metal center (K^{31} coordination mode).

The LnO_9 polyhedra can be best described as monocapped square antiprisms, and, therefore are structurally related to the PbClF structural type.[39-41] The LnO_{10} polyhedra are best represented as bicapped, distorted square antiprisms, similar to compounds **1 – 4** and **9**. Figure **6** shows the resulting coordination network with small sized channels along the *c*-axis that hold numerous interstitial water molecules.
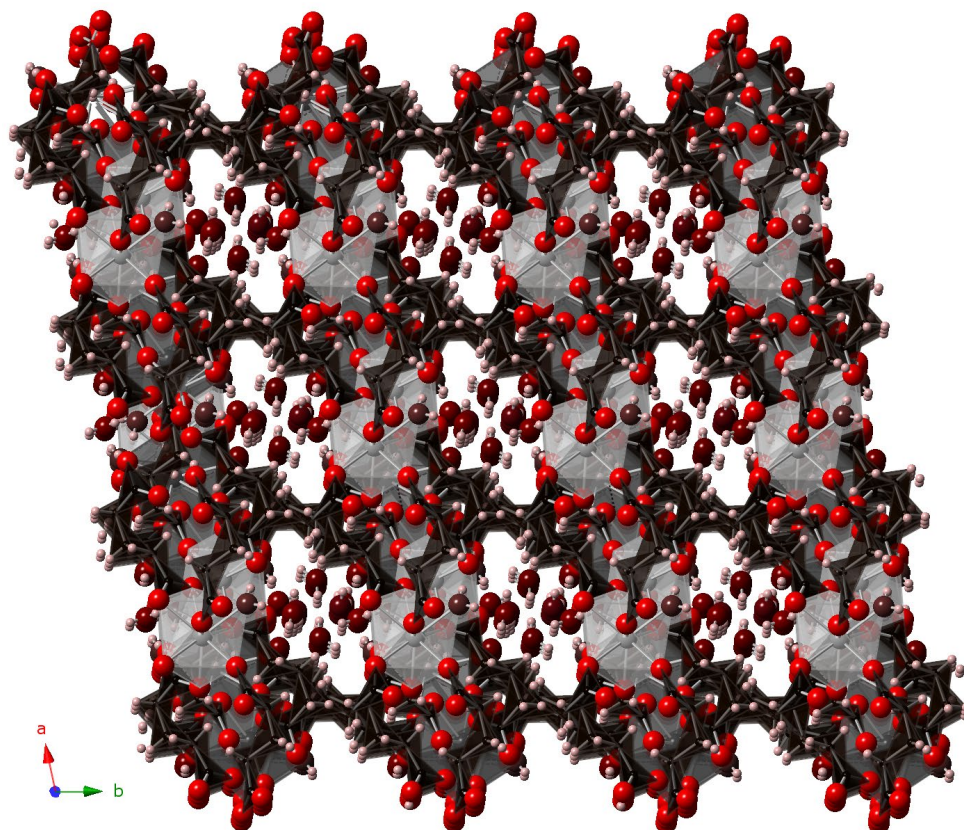
Figure 6. Structural arrangement of **5 - 7**, represented by **6**. The view onto the *ab*-plane shows how LnO_9 and LnO_{10} coordination polyhedra are connected by glutarate units along the *b*-axis rendering the network with small sized cavities filled with water, which could potentially host other small molecules. (red = O, maroon = O (from H_2O), white = H, dark grey = Ln^{3+}-1, light grey = Ln^{3+}-2).

Numerous attempts to crystallize **8** as an isomorphous analogue of **5**, **6**, and **7**, repeatedly resulted in the formation of $[Nd_2(Glut)_3(H_2O)_2] \cdot 3.5H_2O$, crystallizing in the monoclinic crystal system with space group C2/c. As opposed to **5 – 7**, **8** has been previously described by Serpaggi *et al*. and Glowiak *et al*.[32, 33] This neodymium structure is isomorphous with its corresponding Er, Y,[34] Eu, Tb,[36] as well as the Dy[35] analogues. The topology of **8** was found to be a 3,4,5-coordinated 3,4,5T202 net (Figure **7**). This is a topological type not previously described - Serpaggi et al. and Glowiak et al. did not do a topological analysis in their reports – and this type of net has not been reported for a crystal structure before. Coordination modes of the two independent glutarate spacers in **8** are K^{22}, K^{12} (Scheme **1**).
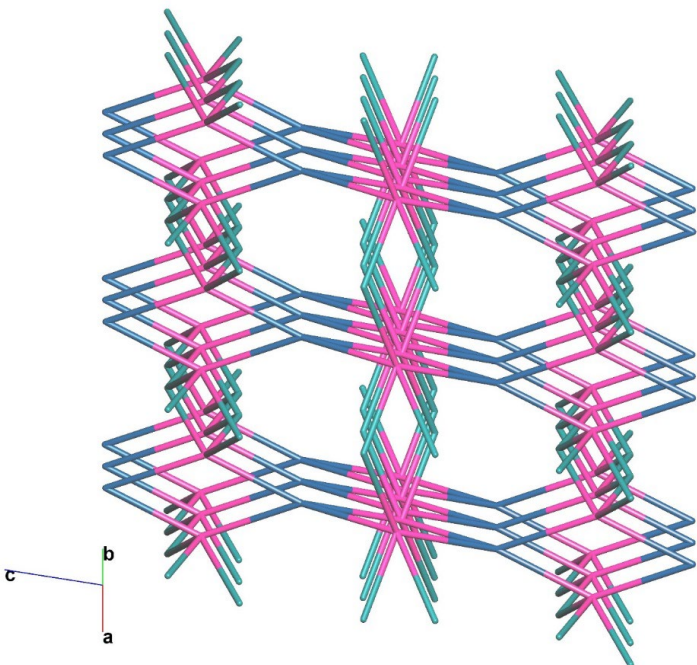
Figure 7. 3,4,5T202 underlying net in the crystal structure of **8**. The underlying net contains 3-, 4- and 5-coordination nodes (cyan, blue and pink colors, respectively).

Comparison of topologies and SBUs

The topological analyses of these compounds and **9** revealed that **1 – 4** have a different overall topology than **9**, classified as a 4,5-coordinated **fsc**-4,5-Cmmm network, shown in Figure 8.
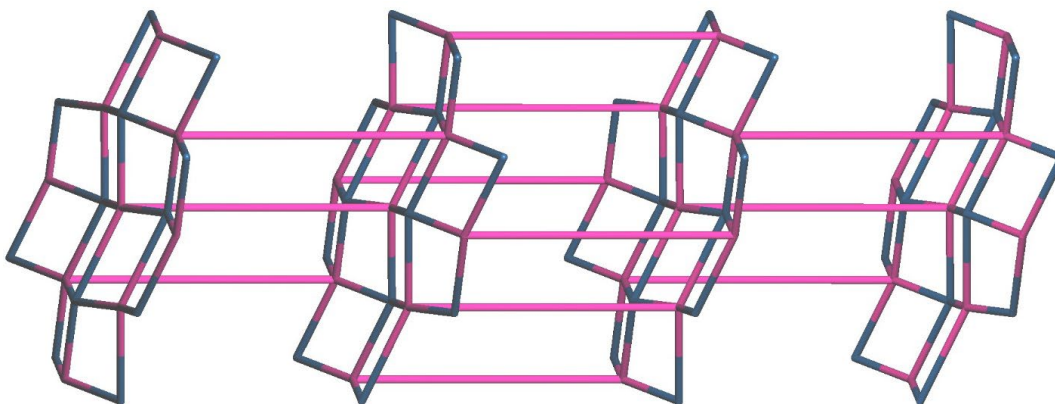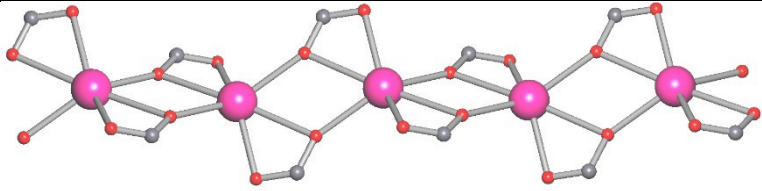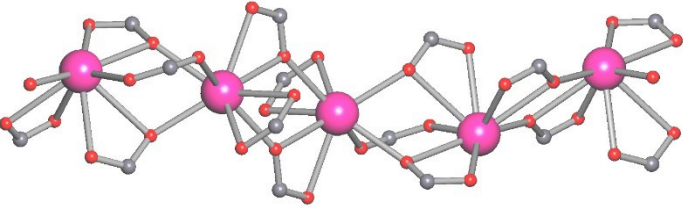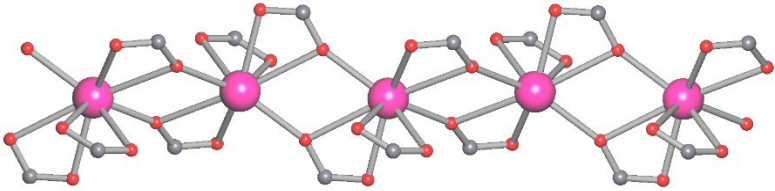

Figure 8. The **fsc**-4,5-Cmmm underlying net in the structure of **9** and homologues, $Ln_2(Glut)_2(TP)(H_2O)_4 \cdot 17H_2O$. The underlying net contains 4- and 5-coordination nodes (blue and pink colors, respectively).

The coordination mode of the glutarate anions is K^{22}, and the coordination mode of the terephthalate units is K^{02} (Scheme **1**). The **fsc**-4,5-Cmmm topology was previously found in a number of crystal structures.[42-47]

The 2D-layers that act as secondary building units, SBUs, in **1 - 4**, were found to be isoreticular with the 2D-layers in **9**. In **1-4** they are tied together by ion-dipole interactions and hydrogen bonds while in **9** and analogues they are interlinked by the terephthalate spacers. Hence, **1 – 4** are directly related to **9** and the fact that they form under the same slow diffusion conditions as **9** indicates that the SBU of **1 - 4** may form in the original reaction mixtures when the TP ligand is present. We propose that the creation of the target compounds proceeds at least in two steps with the 2D-layers in **1 – 4**, composed of $[Ln(Glut)(H_2O)_4]_n$, assembling as SBUs of the glutarate terephthalate network that become then further interlinked via the insertion of the terephthalate ligand. This would take place through the replacement of two coordinating water molecules in the $[Ln(Glut)(H_2O)_4]_n$ SBUs of **1 – 4** with a terephthalate carboxylate unit, resulting in isoreticular $[Ln(Glut)(COO)(H_2O)_2]_n$ SBUs in the corresponding target compounds. Thus, **9** and its analogues seem to be stabilized via the connection of the 2D-SBUs through the terephthalate entities, resulting in water stable 3D-networks. The $[Ln(COO)_2]_n$ rods stretching along *b*-direction in **1 - 4** are subgraphs of the $[Ln(COO)_3]_n$ rods observed in the target compounds as well as in **8**. This relationship can be visualized by comparing the chain structural fragments in Scheme **2**. The chain structural fragments of **1 – 4** lay the foundation for the corresponding fragments in **8** as well as **9**, and analogues as respectively two coordinating water molecules (not shown) become replaced by a carboxylate entity stemming from terephthalate in the target compounds and from glutarate in **8**.

Structure(s)	Fragment	References
1 - 4		Bromant et al.[48] Glowiak et al.[37]
5 - 7		Unprecedented
8 and **target compounds**		Glowiak et al.[32] Wei et al.[35] Serpaggi et al.[33] Yu et al.[36] Bromant et al.[48]

Scheme 2. Characteristic structural moieties in the examined compounds (pink = Ln^{3+}, red = O, grey = C).

The isoreticular 2D-SBUs in **1 – 4** and **9** as well as the related chain structural fragments show that they are the closely related structures, despite the fact that their overall topologies differ. **8** possesses identical chain structural fragments as **9** but does not have the same isoreticular SBUs as found in **1 – 4**. Hence, they are topologically somewhat related to each other but not as closely as **1 - 4** and **9**. The chain structural fragments of **5 – 7** exhibit a completely different topology than **1 – 4**, **8**, or **9**. Thus, there are no commonalities between the overall or SBU topologies in **5 – 7** in comparison with **1 – 4**, **8**, and **9**. In fact, the overall topology in **5 – 7** as well as the topology of their chain structural fragments have been completely unknown,

whereas the chain structural fragments of **1 – 4** have been observed in other networks.[37, 48] The same is true for the topologies of the chain structural fragments in **8** and in **9**.[32, 33, 35, 36, 48]

Since **1 - 4** crystallize out of the THF/EtOH/H_2O solvent mixtures as solid materials we believe that the TP ligand, remaining in solution at first, is then inserted in a rather slow step via replacement of the interstitial Cl^--ions and two water molecules from the coordination spheres, along with an elongation of the interstices along the *a*-axis. While the described slow diffusion syntheses of the target structures proceeds smoothly, attempts to incorporate other dicarboxylic spacer units besides terephthalate or its derivatives in our laboratory have thus far failed. Thus, **1 - 4** may open up avenues to access other targeted mixed ligand Ln-glutarates if a suspension of **1 - 4** in the original mother liquor, THF/EtOH/H_2O, is used as starting material with the described SBUs already preassembled, and brought into contact with a solution of the desired spacer entity. Since the synthesis of **1 – 4** leads to fairly clean products within a reasonable timeframe, when glutarate is used as the only ligand system, this would be a feasible synthetic route to other Ln-glutarate systems incorporating additional organic entities, in which the pore size can be further customized as a function of the chosen dicarboxylic spacer system.

Therefore, in our future investigations we will try to shine more light onto these systems and attempt to confirm our hypothesis. We intend to set up the original reactions for the synthesis of **9** and its analogues, draw samples of crystals formed over time and analyze for the presence of **9** and related materials as well as **1 – 4**. Besides using single crystal X-ray analysis we intend to use FT-IR spectroscopy as an alternative method to detect the insertion of the TP ligand. This is anticipated to work particularly well when using TP derivatives, such as $TPNH_2$ or $TPNO_2$, etc.

CONCLUSIONS

We created a set of new lanthanide glutarate chlorides with THF, and water molecules occupying the interstices. Ln^{3+}-metal centers form LnO_{10} coordination polyhedra, which are related to similar coordination polyhedra we previously found in the compound $[Nd_2(Glut)_2(TP)(H_2O)_4] \cdot 17H_2O$ (**9**).[18] $[Ln(COO)_2]_n$ chains, stretching along the *b*-axis, are tied together by glutarate spacers in *c*-direction. This arrangement results in the assembly of $[Ln(Glut)(H_2O)_4]_n$ SBUs forming 2D-layers in the *bc*-plane. These layers are further connected in *a*-direction, utilizing ion-dipole interactions between interstitial Cl^--ions and coordinating water molecules. The attractive forces between layers are further strengthened via hydrogen bonds between interstitial and coordinating water molecules.

The 2D-layers in **9** possess the same topology as the ones in **1 – 4**, except that in **9** they are further tied into a 3D-network through terephthalate entities along *a*-direction. Thus, **1 – 4** may serve as preassembled SBUs that are required for the production of the targeted 3D-networks via successive insertion of the desired spacer entities. Refining the synthesis for the exclusive preparation of **1 – 4** afforded the described product materials as the only species. Due to the somewhat ionic nature of these compounds **1 – 4** slightly dissolve in water and reassemble as THF and chloride -free lanthanide glutarate hydrates, **5 – 7**, via slow evaporation of water. The small interstices of these frameworks accommodate water molecules. **8** crystallizes differently in the monoclinic crystal system and has been described previously.[32, 33]

We hope that our future investigations will assist with elucidating if **1 – 4** can be utilized as preassembled SBUs for other targeted mixed ligand lanthanide coordination networks, which have been inaccessible to us at this point.

Comparing the topologies of the herein described compounds as well as **9** demonstrated that only structures **1** - **4** have the overall topology (**sql**) that occurs in already published structures. The topological types of **5** – **7** and **8** are unique for glutarates. The type of chains found in **1** - **4** will always result in an **sql** overall topology, while the chains in **8**, and the target compounds are not characteristic and can result in different underlying nets.

ASSOCIATED CONTENT

Supporting Information.

Crystallographic data, CCDC 1558519-1558526, was deposited with the Cambridge Crystallographic Data Centre and can be obtained free of charge via www.ccdc.cam.ac.uk/data_request/cif.

AUTHOR INFORMATION

Corresponding Author

*E-mail: ralph.zehnder@angelo.edu

ORCID: orcid.org/0000-0002-3478-630X

Notes

The authors declare no competing financial interest.

REFERENCES

(1)   Adam, J. L. *Chem. Rev.* **2002**, 102, (6), 2461-2476.

(2)   de Bettencourt-Dias, A.; Barber, P. S.; Bauer, S. *J. Am. Chem. Soc.* **2012**, 134, (16), 6987-6994.

(3)   Luebke, R.; Belmabkhout, Y.; Weselinski, L. J.; Cairns, A. J.; Alkordi, M.; Norton, G.; Wojtas, L. A., K.; Eddaoudi, M. *Chem. Sci.* **2015**, 6, 4095–4102.

(4)   Neogi, S.; Bharadwaj, P. K. *Polyhedron* **2006**, 25, (7), 1491-1497.

(5)   Wang, C. G.; Xing, Y. H.; Li, Z. P.; Li, J.; Zeng, X. Q.; Ge, M. F.; Niu, S. Y. *J. Mol. Struct.* **2009**, 921, 126–131.

(6)   Xue, D. X.; Belmabkhout, Y.; Shekhah, O.; Jiang, H.; Adil, K.; Cairns, A. J.; Eddaoudi, M. *J. Am. Chem. Soc.* **2015**, 137, (15), 5034-5040.

(7)   Zhao, S. N.; Li, L. J.; Song, X. Z.; Zhu, M.; Hao, Z. M.; Meng, X.; Wu, L. L.; Feng, J.; Song, S. Y.; Wang, C.; Zhang, H. J. *Adv. Funct. Mater.* **2015**, 25, (9), 1463-1469.

(8)   Agarwal, R. K. P., J. *Polyhedron* **1991**, 10, (23/24), 2809-2812.

(9)   Bray, T. H.; Gorden, J. D.; Albrecht-Schmitt, T. E. *J. Sol. State Chem.* **2008**, 181, (9), 2199-2204.

(10)   Falaise, C.; Charles, J. S.; Volkringer, C.; Loiseau, T. *Inorg. Chem.* **2015**, 54, (5), 2235-2242.

(11)   Thuéry, P. *Eur. J. Inorg. Chem.* **2013**, 2013, (26), 4563-4573.

(12)   Ziegelgruber, K. L.; Knope, K. E.; Frisch, M.; Cahill, C. L. *J. Sol. State Chem.* **2008**, 181, (2), 373-381.

(13)   Reger, D. L.; Leitner, A. P.; Smith, M. D. *Cryst. Growth Des.* **2016**, 16, (1), 527-536.

(14)   Zhang, Y.; Karatchevtseva, I.; Bhadbhade, M.; Tran, T. T.; Aharonovich, I.; Fanna, D. J.; Shepherd, N. D.; Lu, K.; Li, F.; Lumpkin, G. R. *J. Sol. State Chem.* **2016**, 234, 22-28.

(15)   Chen, F.; Wang, C. Z.; Li, Z. J.; Lan, J. H.; Ji, Y. Q.; Chai, Z. F. *Inorg. Chem.* **2015**, 54, (8), 3829-3834.

(16)   Volkringer, C.; Mihalcea, I.; Vigier, J. F.; Beaurain, A.; Visseaux, M.; Loiseau, T. *Inorg. Chem.* **2011**, 50, (23), 11865-11867.

(17)   Falaise, C.; Volkringer, C.; Vigier, J. F.; Henry, N.; Beaurain, A.; Loiseau, T. *Chem. Eur. J.* **2013**, 19, (17), 5324-5331.

(18)   Zehnder, R. A.; Fontaine, N. C.; Zeller, M.; Renn, R. A. *Acta Cryst. C* **2010**, 66, (12), m371-m374.

(19)   Blatov, V. A.; Shevchenko, A. P.; Proserpio, D. M. *Cryst. Growth Des.* **2014**, 14, (7), 3576-3586.

(20)   O'Keeffe, M.; Peskov, M. V.; Ramsden, S. J.; Yaghi, M. *Acc. Chem. Res.* **2008**, 41, (12), 1782-1789.

(21)   Alexandrov, E. V.; Blatov, V. A.; Kochetkov, A. V.; Proserpio, D. M. *Cryst. Eng. Comm.* **2011**, 13, (12), 3947-3958.

(22)   Serezhkin, V. N.; Vologzhanina, A. V.; Serezhkina, L. B.; Smirnova, E. S.; Grachova, E. V.; Ostrova, P. V.; Antipin, M. Y. *Acta. Cryst. B* **2009**, 65, (Pt 1), B45-B53.

(23)   Sheldrick, G. M.; University of Göttingen, Germany, 2016.

(24)   CrystalClear; Rigaku Corp.: Woodlands, Texas, USA, 2014.

(25)   Otwinowski, Z.; Minor, W., *Methods Enzymol.* In *Macromolecular Crystallography, part A*, Academic Press: New York, 1997; Vol. 276, pp 307-326.

(26)   *SHELXTL (Version 6.14) Bruker Advanced X-ray Solutions*, Bruker AXS Inc.: Madison, Wisconsin: USA., 2000-2003.

(27)   Sheldrick, G. M. *Acta. Cryst.* **2008**, A 64, (1), 112-122.

(28)   Sheldrick, G. M. *Acta Cryst.* **2015**, C71, (Pt 1), 3-8.

(29)   Hübschle, C. B.; Sheldrick, G. M.; Dittrich, B. *J. Appl. Cryst.* **2011**, 44, (Pt 6), 1281-1284.

(30)   SHELXLE Rev656, Rev714 (Hübschle et al., 2011). In ed.

(31)   Sheldrick, G. M. *TWINABS. Ver. 2012/1* **2012**,

(32)   Głowiak, T.; Dao-Cong, N.; Legendziewicz, J. *Acta Cryst. C* **1986**, 42, (11), 1494-1496.

(33)   Serpaggi, F.; Ferey, G. *J. Mater. Chem.* **1998**, 8, 2737-2741.

(34)   Michaelides, A.; Skoulika, S.; Siskos, M. G. *Chem. Commun.* **2013**, 49, (10), 1008-1010.

(35)   Wei, D. Y.; Huang, S. J.; Sun, J.; Zheng, Y. Q. *Z. Kristallogr.* **2006**, 221, (3), 273-274.

(36)   Yu, B.; Xie, C. Z.; Wang, X. Q.; Wang, R. J.; Shen, G. Q.; Shen, D. Z. *J. Coord. Chem.* **2007**, 60, (17), 1817-1825.

(37)   Glowiak, T.; Legendziewicz, J.; Dao, C. N.; Huskowska, E. *J. Less-Common Met.* **1987**, 134, 153-168.

(38)   Vaidhyanathan, R.; Natarajan, S.; Rao, C. N. R. *J. Sol. State Chem.* **2004**, 177, (4-5), 1444-1448.

(39)   Hassan, E. H.; Akbarzadeh, F.; Hashemifar, H.; Mokhtari, A. *J. Phys. Chem. Solids* **2004**, 65, (11), 1871-1878.

(40)   Meyer, G.; Schleid, T. *Z. Anorg. Allg. Chem.* **1986**, 533, 181-185.

(41)   Shen, Y. R.; Englisch, U.; Chudinovskikh, L.; Porsch, F.; Haberkorn, R.; Beck, H. P.; Holzapfel, W. B. *J. Phys. Condens. Matter* **1994**, 6, 3197-3206.

(42)   Adelani, P. O.; Albrecht-Schmitt, T. E. *Inorg. Chem.* **2010**, 49, 5701-5705.

(43)   Bataille, T.; Louër, D. *Acta Cryst. B* **2000**, 56, 998-1002.

(44)   Müller-Buschbaum, K. *Z. Anorg. Allg. Chem.* **2002**, 628, 1761-1764.

(45)   Ouellette, W.; Yu, M. H.; O'Connor, C. J.; Zubieta, J. *Inorg. Chem.* **2006**, 45, (8), 3224-3239.

(46)   Parker, T. G.; Cross, J. N.; Polinski, M. J.; Lin, J.; Albrecht-Schmitt, T. E. *Cryst. Growth Des.* **2014**, 14, (1), 228-235.

(47)   Romero, S.; Mossaet, A.; Trombe, J. C. *Eur. J. Solid State Inorg. Chem.* **1997**, 34, 209-219.

(48)   Bromant, C.; Nika, W.; Pantenburg, I.; Meyer, G. *Z. Anorg. Allg. Chem.* **2005**, 631, (12), 2416-2422.

SYNOPSIS

Lanthanide glutarate chlorides with interstitial THF, $[Ln_2(Glut)_2Cl_2(H_2O)_8]\cdot2H_2O\cdot THF$ (Ln = La, Ce, Pr, Nd) form under similar conditions as target compounds incorporating glutarate and terephthalate, $[Ln_2(Glut)_2(TP)(H_2O)_4]\cdot17H_2O$. Both assemble from identical SBUs.

The glutarate chlorides dissolve in water under loss of THF and convert into glutarate hydrates, $[Ln_2(Glut)_3(H_2O)_3]\cdot5H_2O$ (Ln = La, Ce, Pr) and $[Nd_2(Glut)_3(H_2O)_2]\cdot3.5H_2O$.
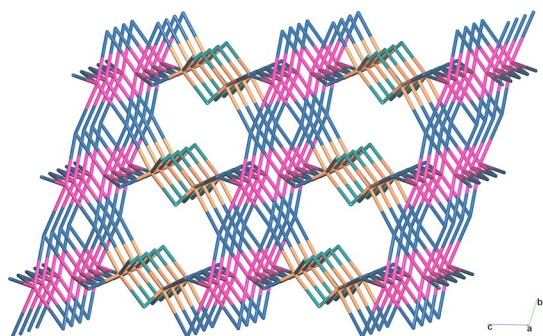
3,4,4,5,6-coordinated 3,4,4,5,6T61 net, an unprecedented topology for $[Ln_2(Glut)_3(H_2O)_3]\cdot5H_2O$, with Ln = La, Ce, Pr, For Table of Contents Use Only